# Facile Fabrication of Hydrophilic Nanofibrous Membranes with an Immobilized Metal−Chelate Affinity Complex for Selective Protein Separation

Jing Zhu and Gang Sun*

Fiber and Polymer Science, University of California, Davis, California 95616, United States

ABSTRACT: In this study, we report a facile approach to fabricate functionalized poly(vinyl alcohol-co-ethylene) (PVA-co-PE) nanofibrous membranes as immobilized metal affinity membranes for selective protein separation. Hydrophilic PVA-co-PE nanofibrous membranes with controlled fiber sizes were prepared via a melt extrusion process. A chelating group, iminodiacetic acid (IDA), was covalently attached to cyanuric acid activated membrane surfaces to form coordinative complexes with metal ions. The prepared membranes were applied to recover a model protein, lysozyme, under various conditions, and a high lysozyme adsorption capacity of 199 mg/g membrane was found under the defined optimum conditions. Smaller fiber size with a higher immobilized metal ion density on membrane surfaces showed greater lysozyme adsorption capacity. The lysozyme adsorption capacity remained consistent during five repeated cycles of adsorption−elution operations, and up to 95% of adsorbed lysozyme was efficiently eluted by using a phosphate buffer containing 0.5 M NaCl and 0.5 M imidazole as an elution media. The successful separation of lysozyme with high purity from fresh chicken egg white was achieved by using the present affinity membrane. These remarkable features, such as high capacity and selectivity, easy regeneration, as well as reliable reusability, demonstrated the great potential of the metal−chelate affinity complex immobilized nanofibrous membranes for selective protein separation.

KEYWORDS: immobilized metal affinity membrane, nanofibrous membrane, hydrophilic, lysozyme, protein separation
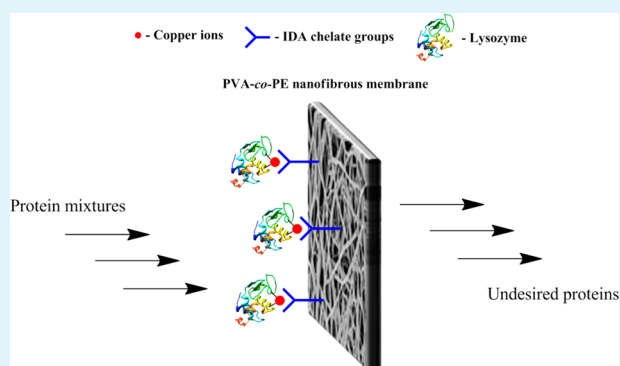
■ INTRODUCTION

Immobilized metal affinity chromatography (IMAC), one of the most powerful methods to separate proteins and enzymes of interest, is based on the coordination reactions between immobilized metal ion−chelate complexes from affinity matrices and electron donor groups from specific amino acids accessible on biomolecule surfaces.[1,2] Owing to its low cost, robustness, simplicity of use, easy regeneration, as well as high binding capacity and selectivity toward target biomolecules with surface-exposed histidine residues, conventional packed column based IMAC is particularly attractive for biological applications and genetic engineering.[3−6] However, this technology suffers inevitable disadvantages including high pressure drop, slow intraparticle diffusion of biomolecules, and difficulty in large column packing, limiting its applications in large-scale separations of protein molecules.[7,8]

To circumvent these general challenges, affinity membranes with immobilized metal ions were explored as an alternative promising technology. The microporous structures of membrane systems and the fine membrane thickness allow high flow rates of protein feed solutions, eliminate large pressure drop, and avoid challenges on column packing.[9−15] Nevertheless, despite these superiorities, the conventional affinity membrane system also has its drawback of relatively low biomolecular binding capacity with respect to the bead-based affinity matrix,

caused by the substantially low surface area of the traditional membrane materials. As an effort to improve protein binding capacity, considerable efforts have been devoted to decorate the surfaces of traditional membranes via grafting polymer chains with multiple binding sites.[16−19] Recent studies reported that a series of polymer brushes, poly(acid),[20,21] poly(2-(methacryloyloxy)ethyl succinate) (poly(MES)),[22] and poly-(2-hydroxyethyl methacrylate) (PHEMA),[23,24] were incorporated onto the surfaces of versatile membrane matrices to achieve enhanced protein binding capacities, respectively. However, extensive growth of polymer brushes may cause clogging of inherent porous structures, leading to an undesired low rate of mass transportation through the system. In addition, the radical polymerization approaches involve multistep reactions on the membranes, which could be a practical concern for large-scale applications.

Nanofibrous membranes would be an attractive alternative to conventional affinity membranes for protein separation due to their extremely high surface areas of nanofibers and open porous web-like structures, enabling high density and easy accessibility of surface active sites and high flow rate of feed

Scheme 1. Immobilization of Chelating Groups (IDA) and Cu²⁺ Ions on the Surfaces of PVA-*co*-PE Nanofibrous Membranes
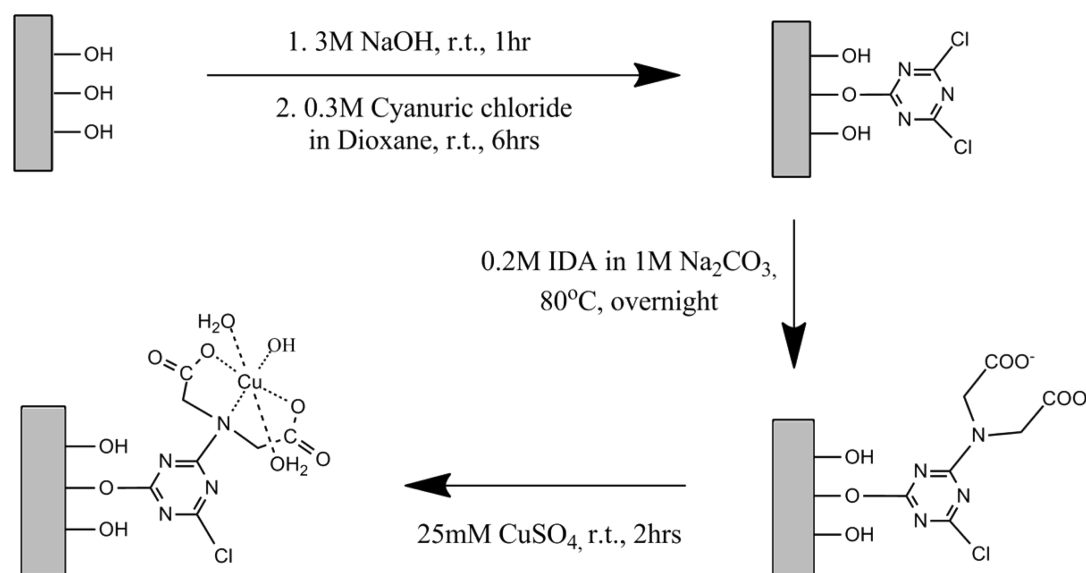
solutions through the membranes. Successful protein separation by using nanofibrous membranes functionalized with affinity dye and recombinant protein ligands has been reported,[25−27] whereas metal ion immobilized nanofibrous membranes as affinity membranes for biomolecular separation have yet to receive any attention. Thus, we herein report the development of hydrophilic nanofibrous membranes with surface immobilized metal ion−chelate complexes for rapid, convenient, efficient, and selective protein separation.

Previously, we reported the successful fabrication and functionalization of poly(vinyl alcohol-*co*-ethylene) (PVA-*co*-PE) nanofibrous membranes for enzyme and protein immobilization.[28,29] The prepared PVA-*co*-PE nanofibrous membrane exhibited high porosity and uniform nanofibrous structures. In addition, its high specific surface area and abundant secondary hydroxyl groups from the alcohol units provided easy access for surface functionalizations with special performances. Most importantly, its hydrophilic surface exhibits excellent resistance to nonspecific protein adsorption, which is a critical property of affinity matrices for separation of biomolecules.[30] These unique features make the PVA-*co*-PE nanofibrous membrane an ideal candidate as immobilized metal affinity membranes for biochromatography applications. Therefore, in this study, PVA-*co*-PE nanofibrous membranes with controlled nanofiber diameters were first prepared as affinity matrixes, which were subsequently functionalized with a chelating group, iminodiacetic acid (IDA), to form coordination complexes with copper ions (Scheme 1). Lysozyme was employed as a model protein to explore the efficacy of the modified nanofibrous membranes in separation and purification of proteins. The effect of nanofiber sizes on surface modifications with the functional moieties and separation of proteins of the prepared membranes were investigated. In addition, the effects of media pH, ionic strength, initial lysozyme concentration, and adsorption time on lysozyme adsorption as well as reusability of the metal ion immobilized PVA-*co*-PE nanofibrous membranes were studied. Direct purification of lysozyme from fresh egg white by the prepared membrane was also evaluated.

■ EXPERIMENTAL SECTION

1. Materials. Poly(vinyl alcohol-*co*-ethylene) (PVA-*co*-PE, 27 mol % ethylene content), cyanuric chloride, iminodiacetic acid (IDA), copper(II) sulfate, imidazole, and lysozyme from chicken egg white (lyophilized powder, protein ≥ 90%, ≥40 000 units/mg of protein) were purchased from Sigma−Aldrich (Milwaukee, WI, USA). Cellulose acetate butyrate (CAB, butyryl content 44−48 wt %), acetone, and dioxane were obtained from Acros Organics (Pittsburgh, PA, USA). Coomassie Brilliant Blue R-250 dyes and Pierce coomassie (Bradford) protein assay kit were purchased from Thermo (Rockford, IL, USA). Buffers were prepared by using analytical grade chemicals, and distilled water was purified via a Millipore Milli-Q plus water purification system.

2. Preparation of the Copper Ion Immobilized PVA-*co*-PE Nanofibrous Membrane. *2.1. Fabrication of PVA-co-PE Nanofibrous Membranes.* PVA-*co*-PE nanofibers were prepared according to a previously published procedure.[31−33] Briefly, PVA-*co*-PE was mixed with CAB as a sacrificial matrix in a blend ratio of CAB/PVA-*co*-PE = 85/15, 90/10, and 95/5, respectively. The blends were gravimetrically fed into a Leistritz corotating twin-screw (18 mm) extruder (model MIC 18/GL 30D, Nurnberg, Germany) at a feed rate of 12 g/min and extruded into composite fibers through a two-strand (2 mm in diameter) rod die, hot-drawn by a take-up device with a drawing ratio of 25 (the area of cross section of the die to that of the extrudates) and air cooled to room temperature. The CAB matrix was removed via Soxhlet extraction of CAB/PVA-*co*-PE composite fibers with acetone. Three grades of PVA-*co*-PE nanofibers prepared from different CAB/PVA-*co*-PE blend ratios at 85/15, 90/10, and 95/5 were designated as PVA-*co*-PE15, PVA-*co*-PE10, and PVA-*co*-PE5, respectively. Then, the prepared nanofibers were made into suspensions and deposited onto a supporting polyester monofilament fabric. After drying in vacuum, free-standing PVA-*co*-PE nanofibrous membranes with controlled thickness were released from the supporting fabrics.

2.2. Immobilization of Chelating Groups and Metal Ions. The chelating group, IDA, and metal ions were immobilized onto the surfaces of prepared nanofibrous membranes according to Scheme 1. To covalently attach the chelating group, 40 mg of PVA-*co*-PE membranes was first soaked in 3 M NaOH at room temperature for 1 h. Then the activated membranes were removed from the alkaline solution and immersed into 0.3 M cyanuric chloride solution in dioxane. After gently shaking for 6 h, membrane samples were thoroughly washed with dioxane and distilled water prior to being placed into 1 M Na₂CO₃ solution, in which 0.2 M IDA was previously dissolved. The mixture was gently shaken overnight at 80 °C, followed

Table 1. Characterizations of PVA-*co*-PE Nanofibrous Membranes with Various Fiber Diameters

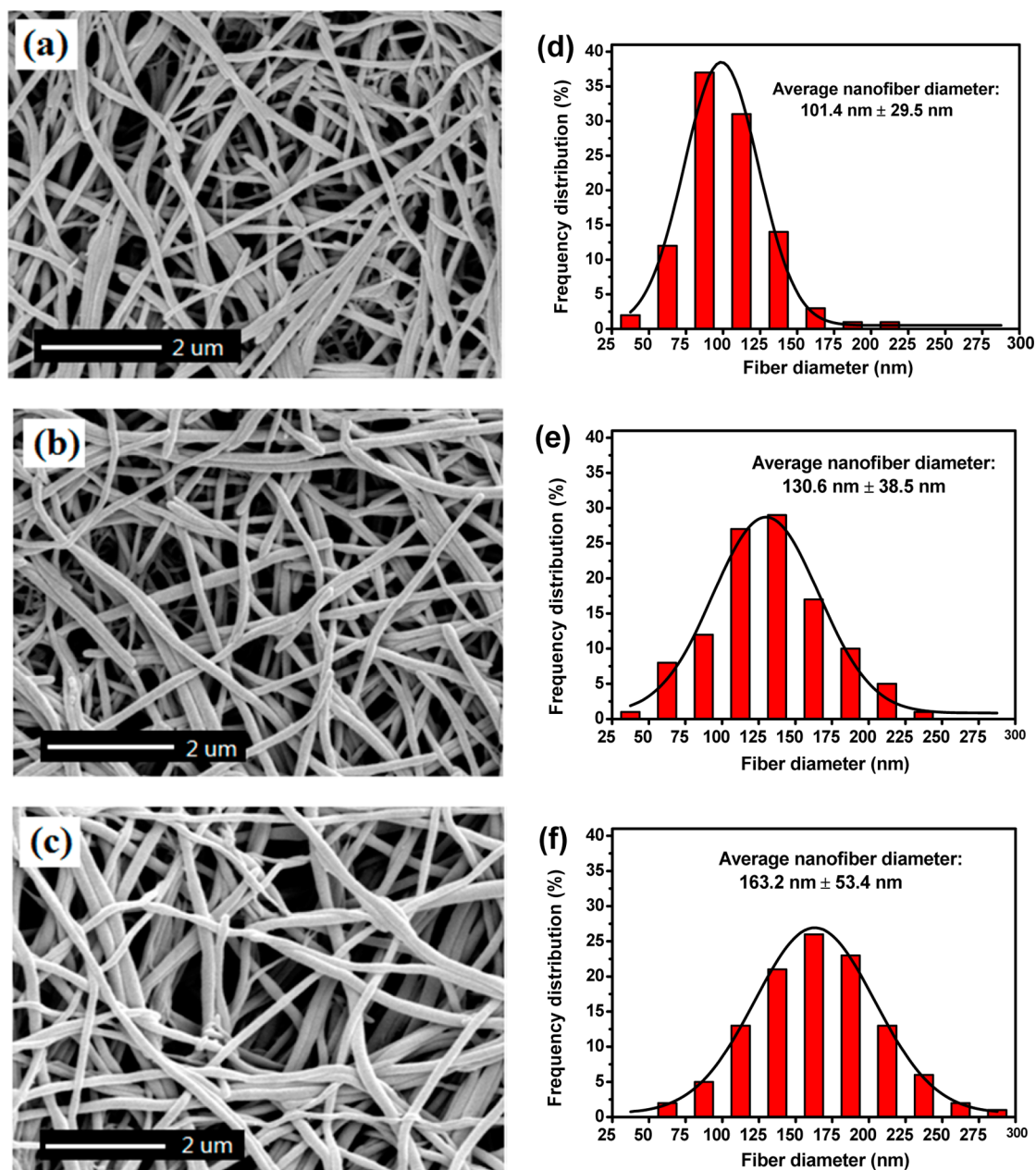| membrane samples	blend ratio (CAB/PVA-*co*-PE)	average fiber diameter (nm)	range of fiber diameter (nm)	hydroxyl groups loading (mmol/g)	copper ion loading (mmol/g)	lysozyme adsorption capacity (mg/g)
PVA-*co*-PE5	95/5	101 ± 29	25–200	9.27 ± 0.66	1.13 ± 0.07	199 ± 6
PVA-*co*-PE10	90/10	131 ± 38	25–250	8.13 ± 0.76	0.98 ± 0.07	167 ± 10
PVA-*co*-PE15	85/15	163 ± 53	50–300	7.28 ± 0.76	0.86 ± 0.08	153 ± 11

Figure 1. SEM images of PVA-*co*-PE nanofibrous membranes: (a) PVA-*co*-PE5, (b) PVA-*co*-PE10, and (c) PVA-*co*-PE15. Fiber diameter distributions of (d) PVA-*co*-PE5, (e) PVA-*co*-PE10, and (f) PVA-*co*-PE15. (Scale bar for SEM images: 2 μm.)

by rinsing with distilled water and acetone to remove any unreacted chemicals.

To form a complex between the immobilized chelating groups and metal ions, the IDA functionalized membranes were immersed into 25 mM $CuSO_4$ solution at room temperature for 2 h according to the literature.[34] Then, the membrane samples were washed with distilled water until no copper ion could be found in washing solutions, followed by drying in vacuum for further experiments. To study the effect of media pH on immobilization of copper ions, the pH values of $CuSO_4$ solution were prepared ranging from 2.0 to 8.0.

2.3. Characterization Methods. The morphology of the nanofibrous membrane was observed by using a scanning electron microscope (SEM) (XL 30-SFEG, FEI/Philips, USA) at 5 kV accelerating voltage on gold sputter-coated samples. Attenuated total reflection-Fourier transform infrared (ATR-FTIR) spectra were measured from 4000 to 500 cm⁻¹ at a resolution of 4 cm⁻¹ by a Nicolet 6700 spectrometer (Thermo Fisher Scientific, USA).

The hydroxyl group loading on the surfaces of PVA-*co*-PE nanofibrous membranes was evaluated via an acetic anhydride/pyridine titration method.[35] Typically, 60 mg of PVA-*co*-PE nano-

927

dx.doi.org/10.1021/am4042965 | ACS Appl. Mater. Interfaces 2014, 6, 925–932

fibrous membranes was immersed into 10 mL of dry pyridine which was previously mixed with 0.2 mL of acetic anhydride. After shaking for 12 h at 50 °C, 2 mL of distilled water was added to convert the excessive acetic anhydride into acetic acid, which was titrated by 0.1 M NaOH, and the titration curves were recorded via a pH meter (848 Titration Plus, Metrohm Swiss). Blank solutions without PVA-*co*-PE nanofibrous membranes were also tested as controls.

The amount of immobilized copper ions on membrane surfaces was determined via measuring UV−vis absorbance.[36] A calibration curve of the absorbance of CuSO$_4$ standard solutions (100 mM EDTA, pH 7.0) was first established by using an UV−vis spectrophotometer (Evolution 600, Thermo, USA) at 730 nm. Then, the copper ions immobilized membrane was immersed in 100 mM EDTA solution (pH 7.0) for 1 h, and the amount of eluted copper ions was evaluated from its absorbance at 730 nm according to the calibration curve. The solutions immersed with original PVA-*co*-PE nanofibrous membranes were tested as controls.

3. Lysozyme Separation Study. *3.1. Lysozyme Static Adsorption Study.* Static lysozyme adsorption capacities on the copper ion immobilized PVA-*co*-PE nanofibrous membranes were performed under varied initial lysozyme concentrations, adsorption time, pH, and ionic strengths of adsorption media. For a typical adsorption test, 20 mg of PVA-*co*-PE5 nanofibrous membrane was placed into 20 mL of lysozyme solution for a certain time at room temperature, followed by an extensive washing with adsorption buffer solution. The lysozyme adsorption capacity was determined by the difference between the initial and final amount of lysozyme in adsorption media, and the concentrations of lysozyme solutions were determined by the Bradford method[37] using a Pierce coomassie protein assay kit. To elute adsorbed lysozyme on membrane surfaces, membrane samples, PVA-*co*-PE5, were immersed into a phosphate buffer (50 mM, pH 8.0) containing 0.5 M imidazole and 0.5 M NaCl for 2 h. The elution efficiency was calculated from the ratio of the amount of desorbed lysozyme and the amount of the adsorbed one. After this elution procedure, the same membrane was placed in 0.1 M EDTA solution to remove immobilized copper ions and rinsed with distilled water. After immersing in 0.5 M NaOH solution for 15 min and thoroughly rinsing with distilled water, the membrane was recharged with fresh copper ions as described above. The adsorption− desorption cycle was repeated up to 5 times.

3.2. Lysozyme Separation from Fresh Chicken Egg White. Prior to lysozyme separation, chicken egg white from fresh chicken eggs was diluted 3 times with a phosphate buffer (50 mM, pH 7.0) and homogenized in an ice bath for 6 h. The resulting solution was further centrifuged (15 000 rpm) at 4 °C for 30 min, and the supernatant was used as the lysozyme resource. Then, 20 mg of the copper ion immobilized PVA-*co*-PE5 nanofibrous membrane was immersed into 20 mL of prepared chicken egg white solution, and the mixture was shaken gently at room temperature for 2 h. After extensive washings with the phosphate buffer, the elution of adsorbed lysozyme on the membrane surfaces was performed in the phosphate buffer (50 mM, pH 8.0) containing 0.5 M imidazole and 0.5 M NaCl. The same membrane was washed and recharged to conduct repeated tests. The purity of eluted lysozyme was examined via sodium dodecyl sulfate polyacrylamide gel electrophoresis (SDS-PAGE) with 12% poly- acrylamide gels with a Pierce unstained protein molecular weight marker (Thermo, Rockford, IL, USA). Coomassie blue staining protocol was employed to visualize the protein bands.[38]

■ RESULTS AND DISCUSSION

1. Preparation of a Copper Ion Immobilized PVA-*co*-PE Nanofibrous Membrane. *1.1. Fabrication of a PVA-*co*-PE Nanofibrous Membrane.* Poly(vinyl alcohol-*co*-ethylene) (PVA-*co*-PE) nanofibrous membranes were first fabricated via melt extrusion of immiscible blends of PVA-*co*-PE and cellulose acetate butyrate (CAB) through a twin-screw extruder, subsequent removal of the CAB matrix, and then an air- spraying process. The unique advantage of this fabrication method is that the control of nanofiber size can be realized by

adjusting the blend ratio of a sacrificial matrix (CAB) and PVA-*co*-PE polymer during the extrusion process. Therefore, PVA-*co*-PE nanofibrous membranes with three different fiber diameters were prepared (Table 1) as an effort to investigate the effect of fiber size on affinity nanofibrous membranes and their applications for protein separation. The morphologies of prepared membranes were observed via SEM. The results in Figure 1(a−c) show that all three membranes exhibit highly open porous nonwoven-like structures with uniform and continuous nanofibers. By using the CAB/PVA-*co*-PE blend ratio at 85/15, the average fiber diameter at 163.2 nm and a broad diameter distribution from 50 to 300 nm were found. Furthermore, the increase of the amount ratio of the sacrificial matrix, CAB, in the immiscible polymer blend system led to reduced fiber size and narrowed diameter distribution. As a result, at the CAB/PVA-*co*-PE blend ratio of 95/5, the finest average fiber size and the most narrow fiber diameter distribution were achieved among the three membrane samples. The same trend was reported before, and the result can be ascribed as a fact of a better dispersion of PVA-*co*-PE in the immiscible polymer composite system by using a smaller amount of PVA-*co*-PE, thus enabling less coalescence of elongated PVA-*co*-PE nanofibrils during the extrusion proc- ess.[39−41]

The feasibility of surface functionalizations on solid materials is mainly determined by the density, reactivity, and accessibility of the reactive sites on material surfaces. The secondary hydroxyl groups from vinyl alcohol segments of the PVA-*co*-PE random copolymer enable a variety of chemical modifications on the materials.[42] Thus, it is necessary to evaluate the hydroxyl group densities on the surfaces of the PVA-*co*-PE nanofibrous membranes. An acetic anhydride/pyridine titration method was conducted for this purpose, and the results are presented in Table 1. The hydroxyl group densities of three PVA-*co*-PE membranes follow the order PVA-*co*-PE5 (9.27 mmol/g) > PVA-*co*-PE10 (8.13 mmol/g) > PVA-*co*-PE15 (7.28 mmol/g), which is consistent with the reverse order of their fiber diameters. This outcome indicates that higher surface area resulted from smaller fiber size and significantly increases the amount of the functional groups on the membrane surfaces.

1.2. Functionalization with Chelating Groups. Iminodi- acetic acid (IDA), one of the most widely used chelating groups for research and commercial products, was selected in this study due to its high coordinative affinity to metal ions, low cost, and convenient availability.[43] The chemical structure changes on three types of PVA-*co*-PE membrane samples after surface functionalizations were observed by ATR-FTIR. Due to the same polymer structure and subsequent surface function- alizations, the identical ATR-FTIR results were found for all three types of membrane samples. Thus, Figure 2 shows the results of PVA-*co*-PE5 membrane samples. In comparison to the PVA-*co*-PE5 original membrane (Figure 2(a)), several new peaks exist in the spectrum of cyanuric chloride activated membranes (Figure 2(b)). The peak at 1545 cm^{-1} is attributed to the stretching of C═N from triazine moieties, and the peaks at 1306 and 1050 cm^{-1} are assigned to C−N of the triazine rings.[44] In addition, the successful coupling of IDA groups onto membrane surfaces was confirmed by the presence of strong peaks at 1585 and 1421 cm^{-1} (Figure 2(c)), the stretching and vibration peaks of dissociated carboxylic acid groups.[45]

1.3. Immobilization of Copper Ions. It is well-known that, after forming complexes with IDA chelating groups, the immobilized copper ions remain two free valencies for
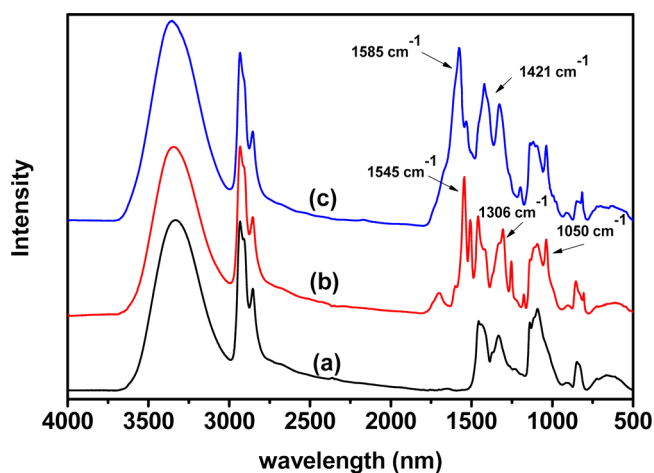
Figure 2. ATR-FTIR spectra of (a) original, (b) cyanuric chloride activated, and (c) IDA attached PVA-*co*-PE5 nanofibrous membranes.

coordination interactions with imidazole rings from histidine residues exposed on protein surfaces.[43] Therefore, the surface density of the immobilized copper ion is crucial for achieving a high protein binding capacity. Here, to optimize the adsorption of copper ions on membrane surfaces, the effect of media pH on copper ion adsorption is studied with pH ranging from 2 to 8. As shown in Figure 3, the amount of adsorbed copper ions
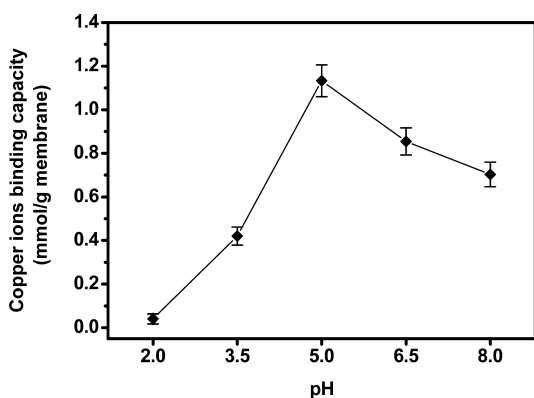

Figure 3. Effect of media pH on Cu^{2+} binding capacity on IDA attached PVA-*co*-PE5 nanofibrous membranes.

on PVA-*co*-PE5 membrane surfaces significantly increases with the increment of media pH and reaches a maximum value at pH = 5. The poor adsorption performance at pH < 5 can be ascribed to the following facts: the dissociation of the weak acid, iminodiacetic acid, becomes more difficult under a higher acidic condition, which results in less binding sites for copper ions on membrane surfaces. Furthermore, more hydrogen ions will protonate the tertiary amines of IDA molecules, causing electrostatic repulsion between metal ions and chelating groups. On the contrary, further increasing media pH value (pH > 5) also leads to a slight decrease of copper ion adsorption, which can be explained by the formed precipitation of complexes between hydroxide ions and copper ions leading to less available copper ions. A similar trend was observed from the other two membrane samples. As a result, pH at 5 is defined as the optimum condition for the following experiments. Under this scenario, the amounts of immobilized copper ions on the surfaces of three PVA-*co*-PE membranes were determined (Table 1). As expected, the membrane sample, PVA-*co*-PE5,

with the smallest fiber size among the three membrane samples exhibited the highest amount of adsorbed copper ion at 1.13 mmol/g, and this value is competitive with respect to other membrane systems reported previously.[36,46,47]

2. Lysozyme Separation Study. *2.1. Lysozyme Static Adsorption Study.* Lysozyme was selected as a model protein to examine the feasibility of the functionalized PVA-*co*-PE membranes for specific protein adsorption. As presented in Figure 4, the original PVA-*co*-PE5 nanofibrous membrane
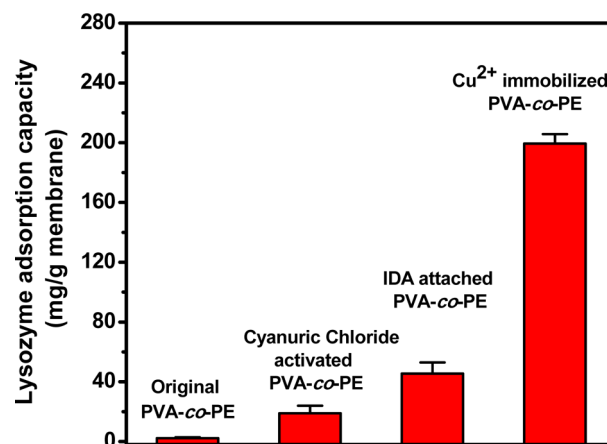

Figure 4. Lysozyme adsorption capacity on original, cyanuric chloride activated, IDA attached, and Cu^{2+} ion immobilized PVA-*co*-PE5 nanofibrous membranes (initial lysozyme concentration: 2 M, adsorption time: 2 h, pH: 7, and no NaCl).

exhibited excellent resistance to nonspecific protein adsorption due to its hydrophilic nature. In comparison to the copper ion immobilized membranes, a small amount of adsorbed lysozyme was found for IDA functionalized membranes, which is a result of electrostatic interactions between the negative-charge-carrying chelating groups and the positive-charge-carrying lysozyme molecules. However, the subsequent formation of a chelating complex with copper ions will significantly reduce the charge density on membrane surfaces and weaken this ionic interaction, thus enabling this nonspecific protein adsorption negligible. PVA-*co*-PE10 and PVA-*co*-PE15 membrane samples also showed a similar trend. Therefore, the high lysozyme adsorption capacity on the copper ion immobilized PVA-*co*-PE nanofibrous membranes is attributed to the specific affinity between the immobilized metal ions and lysozyme molecules.

2.1.1. Effect of pH. Figure 5(a) shows that the effect of media pH on lysozyme adsorption on the copper ion immobilized PVA-*co*-PE nanofibrous membranes is a pH-dependent process. The maximum adsorption capacity was found at pH 7, and this value decreased at either higher or lower pH range. At a low pH range, the electron donor groups on the surfaces of lysozyme molecules may be protonated, which consequently weakens their coordination reactions with immobilized metal ions, whereas, at a high pH range, hydroxide ions and phosphate ions in buffer systems can form complexes with immobilized metal ions and compete with lysozyme molecules for these binding sites. Similar findings were reported previously.[48]

2.1.2. Effect of Ionic Strength. The effect of ionic strength on lysozyme adsorption was evaluated, and the results are shown in Figure 5(b). It is clear that lysozyme adsorption capacity dramatically decreased with the increment of NaCl
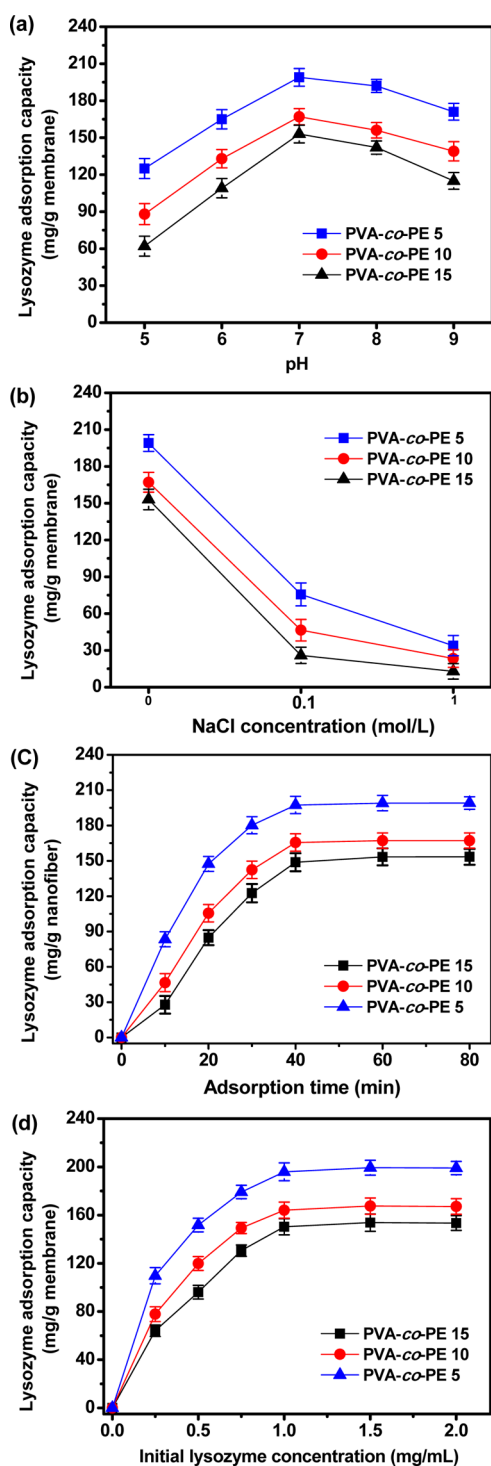
Figure 5. Effects of (a) media pH, (b) ionic strength, (c) adsorption time, and (d) initial lysozyme concentration on lysozyme adsorption.

concentration. When NaCl concentration increased up to 1 M, more than 80% reduction of lysozyme adsorption capacity was observed for all the membranes. The trend is consistent with the observation reported in the literature.[28] This can be explained by the reduced protein solubility in the adsorption media with higher salt concentration. As a result, protein molecules tend to aggregate and shield their surface-exposed electron donor groups and block the reaction with immobilized metal ions. Thus, increasing the ionic strength plays a negative role in lysozyme adsorption.

2.1.3. Effect of Nanofiber Size. In a reasonable agreement with the trends of their surface hydroxyl group loadings and copper ion binding capacities, the lysozyme adsorption capacities on three membrane systems, PVA-*co*-PE5, PVA-*co*-PE10, and PVA-*co*-PE15, were determined as 199, 167, and 153 mg/g, respectively. Once again, this result demonstrates that decreasing fiber diameter improved a higher surface density and enhanced accessibility of the immobilized metal ions to selectively capture target protein molecules. Owing to its highest lysozyme binding capacity, the PVA-*co*-PE5 nanofibrous membrane is employed for further studies on elution and reusability.

2.1.4. Adsorption Kinetics and Isotherm. Under the optimum conditions of the media pH and ionic strength determined above, the amount of adsorbed lysozyme significantly increased initially and then reached an equilibrium after 40 min (Figure 5(c)). At a fixed adsorption time of 60 min, the lysozyme adsorption capacity also increased initially until reaching the plateau value when the initial lysozyme concentration was up to 1.0 mg/mL (Figure 5(d)). Under this scenario, the active binding sites on the membrane surfaces were probably saturated. Thus, further increasing initial lysozyme concentration will not contribute to a higher lysozyme adsorption capacity.

The Langmuir adsorption model illustrates monolayer adsorption of molecules on homogeneous surfaces, which can be expressed by eq 1

$$\frac{1}{q} = \frac{K_d}{q_m \times C} + \frac{1}{q_m} \tag{1}$$

where q_m is maximum adsorption capacity (mg/g); K_d is the dissociation constant of the system (mg/mL); q is the adsorbed lysozyme on nanofibrous membranes (mg/g); and C is equilibrium lysozme concentration (mg/mL). Herein, the inverse equilibrium lysozyme adsorption capacity, $1/q$, is plotted against the inverse equilibrium lysozyme concentration, $1/C$, to investigate the adsorption isotherm of lysozyme on the copper ion immobilized PVA-*co*-PE nanofibrous membranes. As Table 2 shows, the high R^2 values suggest that these

Table 2. Langmuir Adsorption of Lysozyme on Metal-Immobilized PVA-*co*-PE Nanofibrous Membranes

| membrane samples	Langmuir adsorption isotherm		
	maximum adsorption capacity, mg/g (q_m)	dissociation constant, mg/mL (K_d)	R2
PVA-*co*-PE15	221	0.61	0.98
PVA-*co*-PE10	227	0.47	0.97
PVA-*co*-PE5	242	0.29	0.98

lysozyme adsorption isotherms exhibited a typical Langmuir adsorption model. The maximum adsorption capacities (q_m) of lysozyme on the nanofibrous membranes of PVA-*co*-PE5, PVA-*co*-PE10, and PVA-*co*-PE15 were 242, 227, and 221 mg/mL, respectively, which are significantly higher than conventional membrane- and beads-based metal immobilized affinity systems reported previously (Table 3).

2.1.5. Elution and Reusability. Efficient elution and easy regeneration are the essential advantages of immobilized metal affinity chromatography. The adsorbed protein with histidine unit binding can be eluted by introducing high concentrations of salt and imidazole.[49] To evaluate the elution efficiency, the lysozyme adsorbed PVA-*co*-PE5 nanofibrous membrane was

Table 3. Comparison of Lysozyme Maximum Adsorption Capacities on Different Affinity Adsorbents

affinity adsorbents	lysozyme maximum adsorption capacity	reference
lysozyme-imprinted poly(HEMA-MAH) particle	12 mg/g	50
reactive green 19 immobilized membrane	61 mg/mL	51
MAPA ligand attached poly(HEMA) bead	114 mg/g	52
IDA-functionalized PVA-*co*-PE5 nanofibrous membrane	242 mg/g	this study

placed in elution media containing 0.5 M NaCl and 0.5 M imidazole for 2 h, and up to 95% of absorbed lysozyme can be eluted (Figure 6). As an effort to evaluate its regeneration
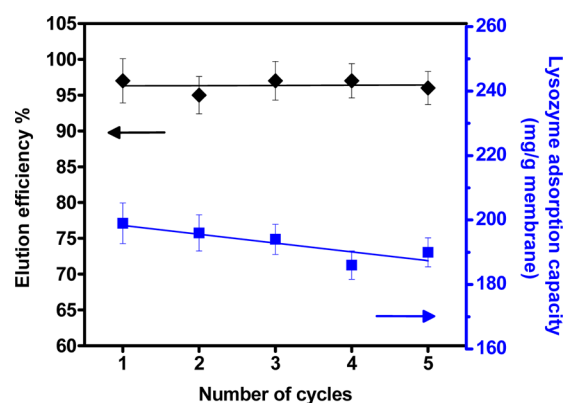
Figure 6. Elution efficiency and lysozyme adsorption capacity of PVA-*co*-PE5 nanofibrous membranes for five adsorption−elution cycles.

efficiency, after each adsorption−elution cycle, the used membrane absorbent was extensively washed and recharged with fresh copper ions for repeated lysozyme adsorption tests. Only slight reduction of lysozyme adsorption capacity (7% of the initial value) was found after five operation cycles (Figure 6). Furthermore, there was no significant change of membrane morphologies after repeated adsorption−desorption experiments, indicating the good durability and reusability of the present PVA-*co*-PE affinity membranes.

2.2. Lysozyme Separation from Fresh Egg White. Lysozyme separation from chicken egg white is the most widely studied model to evaluate the selectivity of immobilized metal affinity absorbents since chicken egg white is composed of a mixture of competitive proteins. In this study, SDS-PAGE was used to determine the purity of eluted lysozyme from fresh prepared diluted chicken egg solution by using the present affinity membrane system. The major protein components, conalbumin, ovalbumin, ovomucoid, and lysozyme with molecular weights at 78k, 45k, 28k, and 14k Dalton, respectively, were detected from nature chicken egg white (Figure 7, Lane 2). However, by using the copper charged PVA-*co*-PE5 nanofibrous membranes, all of the eluates from the membranes exposed to different operation cycles exhibited only one strong protein band (Figure 7, Lanes 3−5), indicating the high purity of eluted lysozyme and confirming the reliable reusability of the present affinity membranes. These remarkable results demonstrate the great potential of the metal ion immobilized PVA-*co*-PE nanofibrous membranes for protein separation applications.
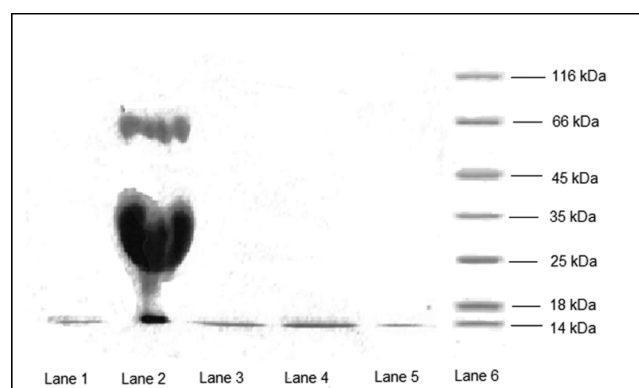
Figure 7. SDS-PAGE analysis of standard lysozyme (Lane 1), protein solution from chicken egg white (Lane 2), and eluted protein solutions from Cu^{2+} immobilized PVA-*co*-PE5 nanofibrous membranes after the 1st (Lane 3), 2nd (Lane 4), and 3rd (Lane 5) operation cycles and standard broad range ladder (Lane 6).

CONCLUSIONS

PVA-*co*-PE nanofibrous membranes with surface attached chelating groups (IDA) and copper ion complexes have been successfully prepared. The possibility of protein separation via the prepared affinity membranes was examined by using lysozyme as a protein model. The inherent enormous surface area and hydrophilic nature enable functionalized PVA-*co*-PE nanofibrous membranes to exhibit high binding capacities toward metal ions and target protein molecules, as well as excellent resistance nonspecific biomolecule adsorption. The optimum condition of lysozyme adsorption on the copper ion immobilized PVA-*co*-PE nanofibrous membrane was determined as the initial lysozyme concentration at 1 mg/mL, adsorption time at 40 min, and adsorption media pH at 7 with no salt. Among the three types of membrane samples, PVA-*co*-PE5, with the finest fiber size presented the highest lysozyme adsorption capacity at 199 mg/g of membrane, up to a 95% desorption ratio of adsorbed lysozyme with only 7% reduction of its initial adsorption capacity after five repeated adsorption−elution cycles. In addition, this affinity membrane allows facilitated separation of lysozyme with high purity from chicken egg white. These features make the metal ion immobilized PVA-*co*-PE nanofibrous membranes very attractive for rapid and efficient protein separation.

AUTHOR INFORMATION

Corresponding Author
*Tel.: (530) 752-0840. Fax: (530) 752-7584. E-mail: gysun@ucdavis.edu.

Notes
The authors declare no competing financial interest.

ACKNOWLEDGMENTS

REFERENCES

(1) Gutierrez, R.; Martin del Valle, E. M.; Galan, M. A. *Sep. Purif. Rev.* **2007**, *36*, 71−111.

(2) Block, H.; Maertens, B.; Spriestersbach, A.; Brinker, N.; Kubicek, J.; Fabis, R.; Labahn, J.; Schäfer, F. *Methods Enzymol.* **2009**, *463*, 439−473.

(3) Gaberc-Porekar, V.; Menart, V. *J. Biochem. Biophys. Methods* **2001**, *49*, 335−360.

(4) Lightfoot, E. N.; Moscariello, J. S. *Biotechnol. Bioeng.* **2004**, *87*, 259−273.

(5) Porath, J.; Olin, B. *Biochemistry* **1983**, *22*, 1621−1630.

(6) Zhang, C. M.; Reslewic, S. A.; Glatz, C. E. *Biotechnol. Bioeng.* **2000**, *68*, 52−58.

(7) Che, S. N.; Liu, Z.; Ohsuma, T.; Sakamoto, K.; Terasaki, O.; Tatsumi, T. *Nature* **2004**, *429*, 281−284.

(8) Zou, H. F.; Luo, Q. Z.; Zhou, D. M. *J. Biochem. Biophys. Methods* **2001**, *49*, 199−240.

(9) Van Reis, R.; Zydney, A. *J. Membr. Sci.* **2007**, *297*, 16−50.

(10) Ghosh, R. *J. Chromatogr. A* **2002**, *952*, 13−27.

(11) Suen, S. Y.; Liu, Y. C.; Chang, C. S. *J. Chromatogr. B* **2003**, *797*, 305−319.

(12) Klein, E. *J. Membr. Sci.* **2000**, *179*, 1−27.

(13) Thommes, J.; Etzel, M. *Biotechnol. Prog.* **2007**, *23*, 42−45.

(14) Brandt, S.; Goffe, R. A.; Kessler, S. B.; O'Connor, J. L.; Zale, S. E. *Biotechnology* **1988**, *6*, 779−782.

(15) Charcosset, C. *Membrane Processes in Biotechnologies and Pharmaceutics*; Elsevier B.V.: Amsterdam, 2012; p 169.

(16) Kawai, T.; Saito, K.; Lee, W. *J. Chromatogr. B* **2003**, *790*, 131−142.

(17) Ulbricht, M.; Yang, H. *Chem. Mater.* **2005**, *17*, 2622−2631.

(18) Yusof, A. H. M.; Ulbricht, M. *Desalination* **2006**, *200*, 462−463.

(19) Hicke, H. G.; Becker, M.; Paulke, B. R.; Ulbricht, M. *J. Membr. Sci.* **2006**, *282*, 413−422.

(20) Dai, J. H.; Bao, Z. Y.; Sun, L.; Hong, S. U.; Baker, G. L.; Bruening, M. L. *Langmuir* **2006**, *22*, 4274−4281.

(21) Anuraj, N.; Bhattacharjee, S.; Geiger, J. H.; Baker, G. L.; Bruening, M. L. *J. Membr. Sci.* **2012**, *389*, 117−125.

(22) Jain, P.; Vyas, M. K.; Geiger, J. H.; Baker, G. L.; Bruening, M. L. *Biomacromolecules* **2010**, *11*, 1019−1026.

(23) Sun, L.; Dai, J. H.; Baker, G. L.; Bruening, M. L. *Chem. Mater.* **2006**, *18*, 4033−4039.

(24) Jain, P.; Sun, L.; Dai, J. H.; Baker, G. L.; Bruening, M. L. *Biomacromolecules* **2007**, *8*, 3102−3107.

(25) Ma, Z. W.; Kotaki, M.; Ramakrishna, S. *J. Membr. Sci.* **2005**, *265*, 115−123.

(26) Ma, Z. W.; Kotaki, M.; Ramakrishna, S. *J. Membr. Sci.* **2006**, *272*, 179−187.

(27) Ma, Z. W.; Ramakrishna, S. *J. Membr. Sci.* **2008**, *319*, 23−28.

(28) Zhu, J.; Yang, J.; Sun, G. *J. Membr. Sci.* **2011**, *385−386*, 269−276.

(29) Zhu, J.; Sun, G. *React. Funct. Polym.* **2012**, *72*, 839−845.

(30) Ghosh, R.; Cui, Z. F. *J. Membr. Sci.* **2000**, *167*, 47−53.

(31) Zhu, J.; Bahramian, Q.; Gibson, P.; Schreuder-Gibson, H.; Sun, G. *J. Mater. Chem.* **2012**, *22*, 8532−8540.

(32) Zhu, J.; Sun, G. *J. Mater. Chem.* **2012**, *22*, 10581−10588.

(33) Zhu, J.; Sun, G. *AATCC Rev.* **2011**, *11*, 62−67.

(34) Ke, Y. M.; Chen, C. I.; Kao, P. M.; Chen, H. B.; Huang, H. C.; Yao, C. J.; Liu, Y. C. *Process Biochem.* **2010**, *45*, 500−506.

(35) Luo, J. T.; Pardin, C.; Lubell, W. D.; Zhu, X. X. *Chem. Commun.* **2007**, *21*, 2136−2138.

(36) Kubota, N.; Nakagawa, Y.; Eguchi, Y. *J. Appl. Polym. Sci.* **1996**, *62*, 1153−1160.

(37) Bradford, M. M. *Anal. Biochem.* **1976**, *72*, 248−254.

(38) Ferraris, M. D. P.; Barrera, G. I.; Padilla, A. P.; Rodríguez, J. A. *J. Chromatogr. B* **2011**, *879*, 2741−2745.

(39) Wang, D.; Sun, G.; Bei, X.; Chiou, B. S. *Eur. Polym. J.* **2008**, *44*, 2032−2039.

(40) Xue, C. H.; Wang, D.; Bei, X.; Chiou, B. S.; Sun, G. *Mater. Chem. Phys.* **2010**, *124*, 48−51.

(41) Xue, C. H.; Wang, D.; Bei, X.; Chiou, B. S.; Sun, G. *J. Polym. Sci., Part B: Polym. Phys.* **2010**, *48*, 921−931.

(42) Avramescu, M. E.; Sager, W. F. C. *J. Membr. Sci.* **2003**, *216*, 177−193.

(43) Wu, C. Y.; Suen, S. Y.; Chen, S. C.; Tzeng, J. H. *J. Chromatogr. A* **2003**, *996*, 53−70.

(44) Karak, N.; Roy, B.; Voit, B. *J. Polym. Sci., Part A: Polym. Chem.* **2010**, *48*, 3994−4004.

(45) Wang, L. J.; Xu, X. Y.; Evans, D. G.; Duan, X.; Li, D. Q. *J. Solid State Chem.* **2010**, *183*, 1114−1119.

(46) Beeskow, T. C.; Kusharyoto, W.; Kroner, K. H.; Deckwer, W. D.; Anspach, F. B. *J. Chromatogr. A* **1995**, *715*, 49−65.

(47) Rodemann, K.; Staude, E. *J. Membr. Sci.* **1994**, *88*, 271−278.

(48) Ergün, B.; Derazshamshir, A.; Odabaşı, M. *Hacettepe J. Biol. Chem.* **2007**, *35*, 143−148.

(49) Kent, M. S.; Yim, H.; Sasaki, D. Y. *Langmuir* **2005**, *21*, 6815−6824.

(50) Odabasi, M.; Say, R.; Denizli, A. *Mater. Sci. Eng., C* **2007**, *27*, 90−99.

(51) Meltem, Y.; Gulay, B.; Arica, M. Y. *Food Chem.* **2005**, *89*, 11−18.

(52) Öncel, S.; Uzun, L.; Garipcan, B.; Denizli, A. *Ind. Eng. Chem. Res.* **2005**, *44*, 7049−7056.